ELSEVIER

Journal of Power Sources 112 (2002) 30–35

JOURNAL OF POWER SOURCES

www.elsevier.com/locate/jpowsour

Synthesis, XRD characterization, and cycling performance of cobalt doped lithium nickelates

R. Moshtev*, P. Zlatilova, I. Bakalova, S. Vassilev

Central Laboratory of Electrochemical Power Sources, Bulgarian Academy of Sciences, Bonchev Street Building 10, Sofia 1113, Bulgaria

Received 9 September 2001; accepted 3 April 2002

Abstract

A simple method for the synthesis of $LiNi_{1-y}Co_yO_2$ with $y = 0.2$–0.3 is developed based on the solid state reaction between LiOH and a mixed oxide precursor, $Ni_{1-y}Co_yO_2$, with a high dispersity and a homogeneous distribution of Ni and Co. The precursor is obtained by ordinary processes, comprising dissolution, evaporation drying and thermal decomposition, avoiding the recently reported sophisticated operations and complex equipment, which makes it viable for industrial application.

The reproducible good values of the XRD criterial parameters $\bar{a}, \bar{c}, \bar{c}/\bar{a}$ and V_h lend evidence for a high stoichiometry and low cation disorder of the samples. The VA-grams of the samples with y above 0.15 reveal that the numerous phase transitions of the $LiNiO_2$ base are reduced to only one, whereby the cycling stability of the cathode material is considerably enhanced.

The discharged capacity of the cathodes with y from 0.2 to 0.30 and with a loading from 15 to 21 mg/cm^2 cycled at the *C*/2 rate (1.2–1.7 mA/cm^2) between 4.30 and 2.80 V varies from 190 to 176 mAh/g at the 10th cycle and reaches 160–165 mAh/g at the 60th cycle.

Keywords: $LiNi_{1-y}Co_yO_2$ cathodes; XRD parameters; Cycling test; VA-metry

1. Introduction

The first samples of $LiNi_{1-y}Co_yO_2$ were synthesized and characterized in detail by Ohzuku et al. [1] in the early 1990s. The electrochemical performance of these samples with $y = 0.25$ and 0.50 was however, inferior to that of the then more investigated $LiNiO_2$.

This explains the loss of interest in Co doped materials until after 1997 when a large number of papers began to appear, disclosing the preparation of Co doped Li nickelates with y up to 0.30 and with superior cycling performance [2–8]. The improvement was achieved by using new starting materials, new precursors, more sophisticated preparation techniques and complex equipment.

The aim of this paper is to elaborate a simple and reproducible method for the synthesis of $LiNi_{1-y}Co_yO_2$ samples with y up to 0.30 possessing charge–discharge characteristics comparable with the best data reported in the recent scientific literature.

2. Experimental

2.1. Preparation and characterization of the precursor

The mixed oxide precursor, $Ni_{1-y}Co_yO_2$ was prepared by simple operations comprising dissolution, evaporation, drying and thermal decomposition using ordinary laboratory apparatuses. The sophisticated processes, requiring complex equipment, described in recent papers [2–8] such as sol–gel procedures, freeze drying, thin layer drying, as well as the additions of noxious organic solvents, or polymer materials were avoided.

A mixed oxide precursor $Ni_{1-y}Co_yO$ was used for the synthesis of the cathode materials. The precursor was prepared by dissolution of appropriate amounts of Ni and Co acetates in dilute acetic acid without any gelling additives. The solution was evaporated and dried. The dry residue was decomposed to the mixed oxide by thermal treatment at 320–400 °C.

The XRD characterization of samples with y up to 0.30 revealed its cubic crystal structure with $\bar{a} = 4.18$ Å equal to that of the undoped NiO. There are no peaks of the CoO phase indicating that the precursor samples are single phase solid solutions with homogeneous distribution of Ni and

* Corresponding author. Tel.: +359-2-722-454; fax: +359-2-722-544.
E-mail address: banchem@bgearn.acad.bg (R. Moshtev).

0378-7753/02/$ – see front matter © 2002 Published by Elsevier Science B.V.
PII: S0378-7753(02)00225-2

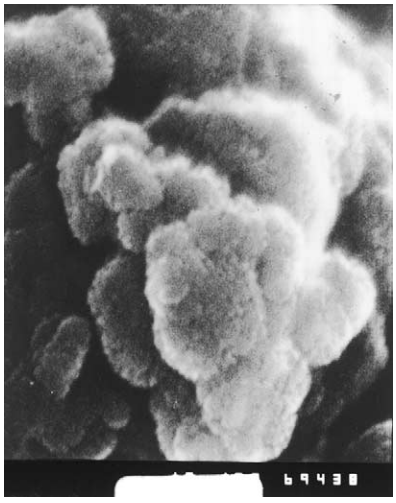

Fig. 1. SEM picture of a precursor sample, $(Ni_{0.75}Co_{0.25})O$ at a magnification of 150,000×.

Co. The full width at half-maximum of the strongest peak of the plane (1 0 4), w(1 0 4), was used as a semiquantitative parameter for the crystallinity of the samples. It was established that precursors with w(1 0 4) in range 1.10–1.20°, 2θ exhibit a large specific area (BET) of 45–50 m^2/g. The SEM picture with a magnification of 150,000× exhibits square platelets with an average size of 0.09–0.10 μm (Fig. 1). It can be assumed that the large surface area of the precursor facilitates its complete solid state reaction with LiOH which can proceed at lower temperatures and shorter annealing time. Under these conditions, the reduction of Ni^{3+} to Ni^{2+} is strongly suppressed and the cation mixing is avoided even in syntheses performed in air atmosphere. The contents of Ni and Co in the precursors as well as in the final products were analyzed by complexometric titration.

2.2. Synthesis and XRD characterization of the $LiNi_{1-y}Co_yO_2$ samples

The carefully mixed LiOH and precursor were pelletized by a slight pressing in the alumina crucible and annealed at temperatures between 680 and 760 °C for 24–14 h under a flow of dry air or oxygen. The starting mixture contained 2–8 at.% excess of LiOH to compensate for the losses by sublimation. The final product was ball milled and sieved. The fine black powder was washed with ethanol to extract the eventual residues of unreacted LiOH.

As in our previous investigations of $LiNiO_2$ [9,10], the Co doped samples were characterized by several XRD parameters. The $\bar{a}$ and $\bar{c}$ distances were estimated from the Bragg angles of the (1 0 8) and (1 1 0) planes (Fig. 2). These values coincided well with those calculated from the data of the nine main peaks in the XRD pattern by the least squares method. As an additional criterion for the stoichiometry of the samples, we employed the integrated intensity ratio $R_d = I(1\,0\,2) + I(0\,0\,6)/I(1\,0\,1)$ introduced by Dahn et al.

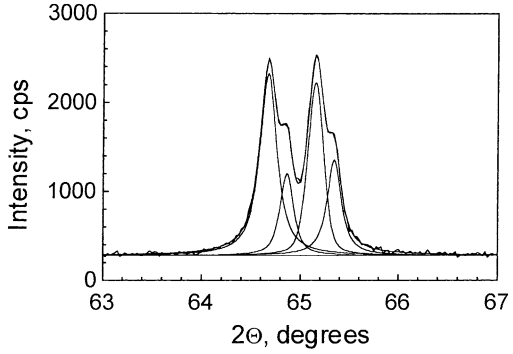

Fig. 2. XRD patterns of the (1 0 8) and (1 1 0) peaks.

[11] for $LiNiO_2$ and later used by several authors (Fig. 3) [3,9,10,12]. The two criterial pair of peaks were recorded on a Philips APD 15 diffractometer with carbon monochromator and Cu Kα radiation using a step size of 0.025°, 2θ and 2 s counting time. The computer collected data were fitted to Gaussian or pseudo-Voigt profiles.

3. Cathodes, cells and cycling conditions

The ball milled powder sample was mixed with 10 wt.% of acetylene black and 5 wt.% of Teflon and the mixture was pressed on thin Al foil discs 15 mm in diameter. The electrochemical behavior of the cathode active material (CAM) depends considerably on the design of the cathode, which is defined by several relevant parameters such as: content and nature of the conductive carbon material and polymer binding material, thickness, loading and apparent density of the pressed cathode, as well as on the porosity, which is closely related to the three former parameters. The method of application of the cathode mixture on the current collector and the conditions of this application (temperature, pressure, retention time) have also certain impact on the final design. In the scientific literature, the cathode design parameters are as a rule not fully described and their values often differ considerably, which makes rather difficult the comparison between the reported electrochemical characteristics of the various CAM's. There are also differences in the

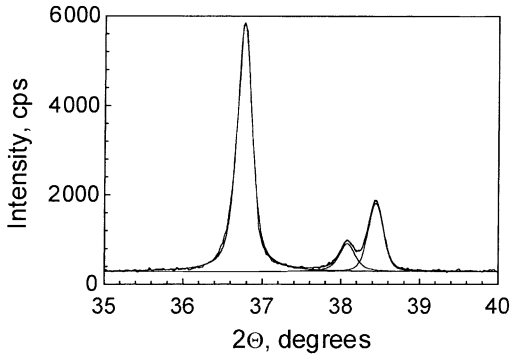

Fig. 3. XRD patterns of the (1 0 1), (0 0 6) and (1 0 2) peaks.

cycling conditions which additionally complicates the correct evaluation of the materials.

It was therefore considered reasonable to accept the average cathode design parameters employed by the five leading Japanese producers of Li-ion batteries described in [13]. These parameters have been, no doubt, optimized as a result of long professional laboratory and mass production experience. The testing of a new CAM in cathodes with these optimized design parameters can allow for a more realistic evaluation of its electrochemical (EC) characteristics.

In our EC experiments, we used cathodes with design parameters close to the optimized ones: thickness 75–90 μm, loading 17–20 mg/cm^2, apparent density 2.4–2.6 g/cm^3, and a porosity in the 40–43% range. After drying in vacuum at 150 °C, the cathodes were assembled in stainless steel laboratory cells with a Li metal anode and a Li/Li$^+$ reference electrode positioned close to the cathode. The electrodes were separated by two sheets of glass fiber paper Amer-Sil. The electrode pack was subjected to a slight pressure by a steel spring in order to suppress the formation and growth of dendrites on the Li anode and improve the contact between the electrodes. All assembly operations were conducted in a dry box with less than 20 ppm of water. One molar $LiClO_4$ solution in EC + PC (1:1) with less than 20 ppm of water was used as electrolyte.

The cycling procedure was also similar to that practiced by the leading Japanese producers [13]. It will be described in more detail in Section 4.

4. Results and discussion

4.1. XRD characterization

Typical XRD criterial parameters of $LiNi_{1-y}Co_yO_2$ samples with y from 0.20 to 0.30 synthesized at 720 and 760 °C are shown in Table 1. The data reveal that irrespective of the differences in the Co content and the synthesis temperatures the lattice parameters are quite similar and the values are among the best ones recently reported in the literature [2–8]. More specifically, the low values of the $\bar{a}$ and $\bar{c}$ distances and of the hexagonal unit cell volume, V_h, as well as the large value of the $\bar{c}/\bar{a}$ ratio lend evidence for samples with a low cation disorder and high stoichiometry. The latter is also exhibited by the low values of the R_d integrated intensity ratio. According to [11], R_d of the perfectly stoichiometric $LiNiO_2$ is 0.411. It was shown later that Li_xNiO_2 samples with $R_d = 0.397$ are overlithiated with $x = 1.02$ [9,10,14]. There are no literature data for R_d of $LiCoO_2$ or of Co doped Li nickelates. It was established experimentally in our laboratory that the R_d of a high stoichiometry $LiCoO_2$ is 0.420. It is reasonable therefore to assume that the low R_d values of 0.37–0.39 of the present Co doped samples (Table 1) with prevailing Ni content can serve as a reliable indication for their high stoichiometry.

4.2. Morphology

The SEM observation of the samples at lower magnifications (1000–5000×) display crystal aggregates with dimensions of several tens of microns. The SEM pictures in Fig. 4 with a larger magnifications (60,000×) illustrate the morphology of the crystallites forming the aggregates of two samples with $y = 0.25$ obtained at 720 and 760 °C, respectively. The well polygonized hexagonal platelets of both samples are typical for the rhombohedral crystal lattice of the $R\bar{3}m$ space group. The smaller crystallites of the sample synthesized at 720 °C with a size of 0.2–0.3 μm have a specific surface area (BET) of 2.0–2.5 m^2/g. It can be expected that this cathode material could yield a larger power capability and will operate better at sub-zero temperatures. On the other hand, the large specific surface area enhances the chemical reactivity with the organic solvents leading to an increased self-discharge and a lower safety under abuse conditions. The opposite will be true for the samples obtained at 760 °C with larger crystallites of 1.0–1.2 μm and a surface area of 0.6–0.8 m^2/g, which supposes a lower chemical reactivity combined with a lower power capability. The choice between these two types of materials will depend on the prevailing exploitation conditions of the battery.

4.3. Cycling performance

Fig. 5 presents typical charge–discharge voltage profiles together with the corresponding current–time plots of a Li/$LiNi_{1-y}Co_yO_2$ cell cycled between 2.80 and 4.30 V at the fifth cycle. The charging current of 80 mA/g or 1.50 mA/cm^2 is constant to the upper limiting voltage of 4.30 V after

Table 1
Criterial XRD parameters of $LiNi_{1-y}Co_yO_2$ samples

No.	y	LiOH (excess %)	t_s (°C)	τ_s (h)	$\bar{a}$ (Å)	$\bar{c}$ (Å)	$\bar{c}/\bar{a}$	R_d	Å^3
1	0.20	3	720	22	2.862	14.158	4.947	0.395	100.4
2	0.25	5	720	24	2.860	14.147	4.947	0.376	100.2
3	0.28	6	720	22	2.860	14.148	4.947	0.396	100.2
4	0.20	6	760	14	2.863	14.157	4.945	0.369	100.5
5	0.25	7	760	14	2.860	14.150	4.947	0.380	100.2
6	0.28	6	760	15	2.859	14.152	4.950	0.379	100.2

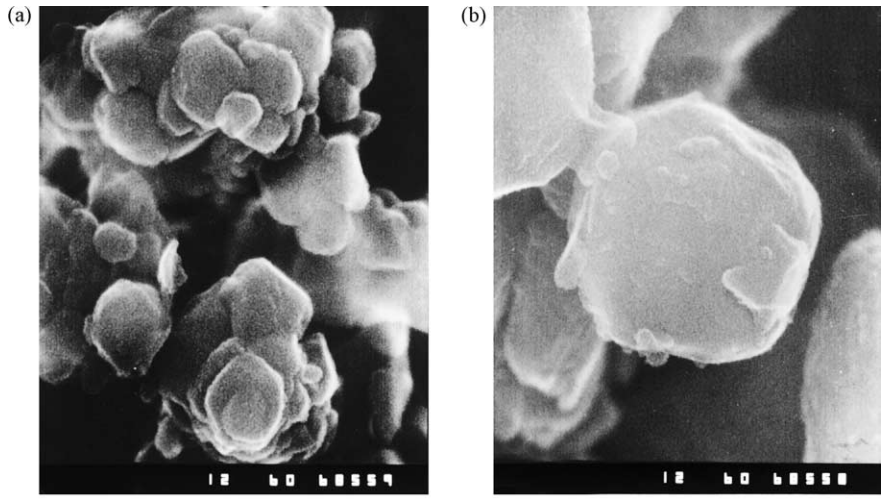

Fig. 4. SEM micrographs of two $LiNi_{0.75}Co_{0.25}O_2$ at: (a) 720 °C and (b) 760 °C at a magnification 60,000×.

which the latter is maintained constant while the charging current decreases exponentially to a predetermined minimum of 0.10–0.15 mA/cm^2. The cell is then switched automatically to galvanostatic discharge at 40 mA/g or 0.75 mA/cm^2 corresponding to the *C*/4.5 rate. A characteristic feature of this mode of charging is the relative state of charge, x_c, at the end of the constant charging to 4.30 V, expressed by the ratio:

$$x_c = \frac{q_{c,1}}{q_{c,1} + q_{c,2}},$$

where $q_{c,1}$ is the charge capacity accumulated during the constant current charging and $q_{c,2}$ is the additional capacity obtained during the constant voltage charging, which is estimated by integration of the respective current–time plot. A large x_c indicates the ability of the cathode to be almost completely charged at the high charging current and also implies a large power capability of the cathode during discharge. For a given cathode design, the value of x_c could determine the quality of various cathode active materials. On the other hand, the comparison of the x_c values of a series of cathodes with one and the same cathode active material could be used to optimize the cathode design parameters by their variation.

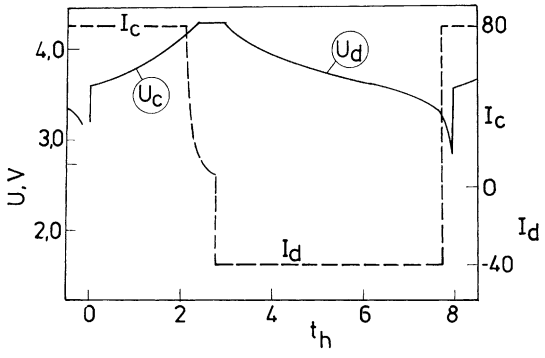

Fig. 5. Typical charge–discharge voltage profiles and the corresponding current–time plots of a Li/ $LiNi_{0.75}Co_{0.25}O_2$ cell, charged at 80 mA/g (1.50 mA/cm^2) and discharged at 40 mA/g (0.75 mA/g) at the fifth cycle.

In the example in Fig. 2 $x_c = 0.93$ remained constant during 30 cycles. The discharge rate of the cell was then raised to *C*/2 whereupon x_c began slowly to decrease, reaching 0.89 after 60 cycles. It is noteworthy that the x_c value of the non-doped $LiNiO_2$ cathodes is considerably lower than those of the Co doped. It was shown earlier [10] that x_c even of the high stoichiometry $LiNiO_2$ cathodes is only 0.75–0.78, which reflects their poorer power capability compared to that of the Co doped cathodes.

Table 2 illustrates the decrease in the discharge capacities q_d with the number of cycles of five $LiNi_{1-y}Co_yO_2$ cathodes with different Co contents and different loadings charged and discharged at 80 mA/g or at *C*/2. It is seen that the cathode with the lowest loading of 15 mg/cm^2, respectively with the lowest c.d. exhibits the largest q_d values in the first 30 cycles but after 60 cycles, its capacity becomes similar to those of the cathodes with the larger loadings. At the 60th cycle, the capacities of all the cathodes are very similar irrespective of their different Co content and loading.

Table 2
Discharge capacities of five $LiNi_{1-y}Co_yO_2$ cathodes with different Co contents, *y* and various loadings as a function of the number of cycles at *C*/2 rate

No.	*y*	Loading (mg/cm^2)	i_d (mA/cm^2)	Discharge capacity (mAh/g) at cycle number				
				10	20	30	50	60
1	0.20	15	1.2	192	184	178	170	164
2	0.25	16	1.3	180	173	173	164	160
3	0.25	21	1.7	176	172	172	171	168
4	0.30	17	1.4	176	171	165	163	158
5	0.30	18	1.5	176	173	173	168	165

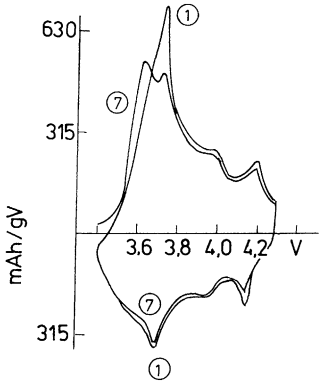

Fig. 6. VA-gram of a $LiNi_{0.85}Co_{0.15}O_2$ cathode recorded with a scan rate of 50 mV/h.

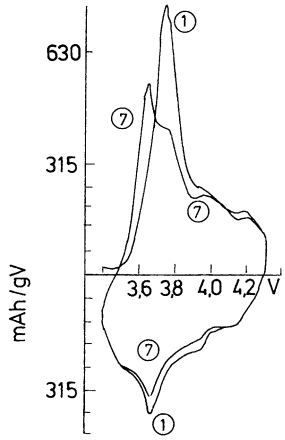

Fig. 7. VA-gram of a $LiNi_{0.70}Co_{0.30}O_2$ cathode recorded with a scan rate of 50 mV/h.

4.4. Cycling voltammetry

In spite of its larger discharge capacity of 180–200 mAh/g $LiNiO_2$, could not acquire practical application as a cathode material in the Li-ion commercial batteries mainly because of its unsatisfactory cycling stability. On the other hand, $LiCoO_2$ with a lower discharge capacity of 150–160 mAh/g and higher price remains still the only cathode material in these batteries thanks to its excellent cycling and better thermal stability. The instability of $LiNiO_2$ is related to the large number of phase transitions occurring during the cycling process, some of which are accompanied by considerable changes in the crystal lattice. In contrast, the discharge capacity of $LiCoO_2$ is obtained by a single phase transition exhibited in the VA-gram by a single peak at 3.93 at charge and at 3.92 V at discharge [14]. The introduction of Co in $LiNi_{1-y}Co_yO_2$ solid solution with y from 0.15 to 0.30 preserves the inherent high discharge, capacity of $LiNiO_2$ and in the same time improves its stability by suppressing most of the phase transitions.

Fig. 6 presents the first and the seventh VA-gram of a $LiNi_{0.85}Co_{0.15}O_2$ cathode recorded at 50 mV/h scan rate between 3.40 and 4.30 V. In the first charging half-cycle, there appears a high sharp peak at 3.75 V, which in the second cycle is split into two lower peaks at 3.64 and 3.75 V. Above 3.80 V, the charging current is slowly decreasing and one can see a low round peak at ca. 4.0 V and a low sharp peak at 4.20 V, which pertain to the R_2 and R_3 hexagonal phases of $LiNiO_2$. In the next cycles, of which only the seventh is shown, all the features of the second charging half-cycle are closely reproduced, which implies an improved cyclability. The discharge peaks of these VA-grams are similar in position to those in the charging ones. The reappearance of the unstable R_3 phase at 4.20 V, however, is an indication for a limited improvement of the cycling stability of this low Co content cathode material.

The VA-gram in Fig. 7 of a $LiNi_{0.70}Co_{0.30}O_2$ cathode in the first charging half-cycle displays a very high sharp peak at 3.75 V. In the next cycle, this peak is split into a lower sharp peak at 3.64 V and a shoulder at 3.74 V. Above 3.80 V, the charging current steadily falls but in contrast to the low Co content cathode in Fig. 6 the lower peaks at 4.0 and 4.20 V are hardly visible. The VA-grams of the second cycle are here again closely reproduced to the seventh cycle. Actually, after the third cycle, the VA-grams display only one charging peak at 3.64 V and a broader discharging peak at 3.66 V. The small difference between these two voltages exhibits the good reversibility of this cathode.

The comparison between the VA-grams in Figs. 6 and 7 shows that the increase of Co above 0.15 transforms the cathode material from three phase to a single phase one, which is a condition for a much better cycling stability. It is worth noting that the charge/discharge peaks of the Co-rich cathode after the third cycle have the same positions as those of $LiNiO_2$ at 3.65 and 3.60 V, respectively. This similarity indicates that the larger part of the capacity of this cathode is delivered by the oxidation and reduction of the Ni^{3+} ions, while the capacity contribution by the oxidation of the Co^{3+} ions is very small. Such a supposition is supported by the recent results of Montoro et al. [15] by X-ray absorption spectroscopy that during the oxidation of $LiCoO_2$ the Co^{3+} ions are not oxidized to Co^{4+} and that the electrons released during the oxidation reaction are provided from the partial oxidation of the oxygen ions to O_2.

5. Conclusion

A simple method for synthesis of $LiNi_{1-y}Co_yO_2$ samples with y from 0.20 to 0.30 is described, based on the solid state reaction between LiOH and a mixed oxide precursor $(Ni_{1-y}Co_y)O$. The precursor exhibits a high specific surface area, 45–50 m^2/g, and a homogeneous distribution of Ni and Co, which enhances its complete reaction with LiOH at comparatively lower temperatures and shorter annealing times. By reasonable adjustment of the synthesis conditions, it was possible to obtain at 720 and 760 °C, quality samples with very close and reproducible XRD criterial parameters: $\bar{a} = 2.861 \pm 0.001$ Å, $\bar{c} = 14.152 \pm 0.004$ Å, $\bar{c}/\bar{a} =$

4.947 ± 0.001, and $V_h = 100.2 \pm 0.002$ Å, which reveal the high stoichiometry and low cation disorder in the rhombohedral crystal lattice. The SEM pictures at a magnification of 60,000× display hexagonal platelets with an average size of 0.2–0.3 μm for the samples obtained at 720 °C and of 1.0–1.2 μm for those obtained at 760 °C. The comparison between the VA-grams of non-doped $LiNiO_2$ and of $LiNi_{0.70}Co_{0.30}O_2$ show that the numerous phase transitions of $LiNiO_2$ are strongly suppressed so that the VA-gram of the Co substituted cathode displays a single phase which imparts an improved cycling stability. Cathodes with $y = 0.25$ discharged at the *C*/2 rate between 4.30 and 2.80 V yield 190–176 mAh/g at the 10th cycle and 160–165 mAh/g after 60 cycles.

References

[1] T. Ohzuku, A. Ueda, M. Nagayama, I. Iwakishi, H. Komori, Electrochem. Acta 38 (1993) 1159.
[2] W. Li, J. Curie, J. Electrochem. Soc. 144 (1997) 2773.
[3] Y. Fujita, K. Amine, J. Maruta, H. Yasuda, J. Power Sources 68 (1997) 126.
[4] C. Chang, P. Kumta, Ibid. 75 (1998) 44.
[5] K. Kubo, S. Arai, S. Yamada, M. Kanda, Ibid. 81/82 (1999) 599.
[6] G. Wang, J. Horvat, D. Brandhurst, H. Liu, S. Dou, Ibid. 85 (2000) 279.
[7] J. Cho, G. Kim, H. Lim, J. Electrochem. Soc. 146 (1999) 3576.
[8] R. Gover, R. Kanno, B. Mitchel, M. Yonemara, Y. Kawamoto, J. Electrochem. Soc. 147 (2000) 4045.
[9] R. Moshtev, P. Zlatilova, S. Vassilev, I. Bakalova, K. Tagawa, A. Kozawa, Prog. Batteries Battery Mater. 16 (1997) 268.
[10] R. Moshtev, P. Zlatilova, S. Vassilev, I. Bakalova, A. Kozawa, J. Power Sources 81/82 (1999) 434.
[11] J. Dahn, U. von Sacken, C. Michal, Solids State Ionics 44 (1990) 87.
[12] J. Reimers, J. Dahn, J. Greedan, C. Stager, G. Lui, I. Davidson, U. von Sacken, J. Solid State Chem. 102 (1993) 542.
[13] R. Moshtev, B. Johnson, J. Power Sources 91 (2000) 86.
[14] W.S. Yoon, K.B. Kim, J. Power Sources 81/82 (1999) 517.
[15] L.A. Montoro, M. Abate, J.M. Rosolen, Electrochem. Solid State Lett. 3 (9) (2000) 410.